COMPARATIVE STUDY OF COMPENSATION MECHANISM OF LUNAR IMPACT BASINS FROM NEW GRAVITY FIELD MODEL OF SELENE (KAGUYA).

N. Namiki[1], S. Sugita[2], K. Matsumoto[3], S. Goossens[3], Y. Ishihara[3], H. Noda[3], S. Sasaki[3], T. Iwata[4], H. Hanada[3], H. Araki[3], K. Kurosawa[2], M. Matsumura[4], M. Yokoyama[2], S. Kamata[2], N. Kubo[1], A. Mori[1], and M. Sato[1], [1]Kyushu University (6-10-1 Hakozaki, Higashi-ku, Fukuoka 812-8581, Japan; nori@geo.kyushu-u.ac.jp), [2] The University of Tokyo (5-1-5 Kashiwanoha, Kasiwa, Chiba, 277-8561, Japan), [3]National Astronomical Observatory of Japan (2-12 Hoshigaoka, Mizusawa, Oshu, Iwate 023-0861, Japan), [4]Institute of Space and Astronautical Science, Japan Aerospace Exploration Agency (3-1-1 Yoshinodai, Sagamihara, Kanagawa 229-8510, Japan).

Introduction: The gravity field is a fundamental physical quantity for the study of the internal structure and the evolution of planetary bodies. In 1966, the Luna 10 mission began the study of the gravity field from observed orbital motion of the spacecraft. Muller and Sjogren [1] discovered large positive gravity anomalies called "mascons" within maria basins on the near side. The elliptic orbit of the Clementine spacecraft improved the lower degrees and sectorial terms of the gravity field [2]. The low circular, polar orbit of Lunar Prospector increased the spatial resolution of the near side gravity field [3].

The most significant problem of the previous lunar gravity models is the lack of direct observations of the far side gravity signals [3]. Synchronous rotation of the Moon with its orbit inhibits a direct link between an Earth-based ground tracking station and a lunar-orbiting spacecraft over the far side. Consequently, about one third of the lunar surface remains uncovered by direct tracking data. In order to compensate for the lack of tracking data on the far side, an a priori constraint [4] has been used in processing tracking data to produce a global lunar gravity field model [2, 3, 5, 6]. However, the far side gravity field will remain unresolved until global coverage of gravimetric observations is achieved. We then developed a satellite-to-satellite Doppler tracking sub-system for SELENE [7]. Preliminary results of our gravity experiment were argued by Namiki et al. [8]. In this study, we adopt our new gravity field model with nearly full coverage of the lunar far side to discuss dichotomy of the lunar basins.

Because all the nearside impact basins are filled with extensive mare basalt deposits, it is difficult to estimate the subsurface structures, such as uplift of the Moho surface, from gravity measurements. In contrast, far-side impact basins have much less mare basalt coverage, often none. This may allow us to investigate the internal structure underneath impact basins. Such knowledge will be important in understanding the response of a solid planetary body to large meteoritic impacts and also the thermal state of the Moon during the late heavy bombardment period. Thus in this study, we investigate the internal structures of large impact basins using our newly obtained gravity data.

New Gravity Field Model: We estimated a new spherical harmonic model of the lunar gravity field, complete to degree and order 90, from the data sets, designated SGM90d (SELENE Gravity Model with the maximum degree and a version number). On the near side, a comparison with a previous lunar gravity model reveals general agreement. The five principal gravity highs on Imbrium, Serenitatis, Crisium, Nectaris, and Humorum are clearly visible, as in the previous models. On the far side, in contrast, the gravity field model shows several circular signatures that correspond to topographic structures such as Moscoviense, Freundlich-Sharonov, Mendeleev, Hertzsprung, Korolev and Apollo basins unlike linear signatures in previous models [9].

Classification of Lunar Basins: There are distinctive differences between the anomalies of the near side principal mascons and the far side basins. As shown previously [2, 3], the near side principal mascons have sharp shoulders with a gravity plateau and a weakly negative gravity anomaly in the surroundings (Fig. 1a). In contrast, the far side basins are characterized by concentric rings of positive and negative anomalies. The circular gravity highs agree well with the topographic rims of the basins revealed by STM-359_grid-02 [10]. In our gravity model, Orientale, Mendel-Rydberg, Lorentz, and Humboldtianum show more affinity with the far side basins than the near side principal mascons [9].

Korolev (Fig. 1b), Mendeleev, Planck, and Lorentz basins have sharp central peaks of which magnitude in free-air anomalies is almost equivalent to the one in Bouguer anomalies. On the other hand, Orientale, Mendel-Rydberg, Humboldtianum, Moscoviense (Fig. 1c), and Freundlich-Sharonov basins have a broad peak of which magnitude in free-air anomalies is 20 to 60 % smaller than the one in Bouguer anomalies. We call the former basins Type I and the latter Type II. Most Type II basins, except for the Hertzsprung basin, are associated with mare fill, for example, in Orientale, Mendel-Rydberg, Humboldtianum, Apollo, and Moscoviense basins [11, 12]. The Freundlich-Sharonov basin has been regarded to have only a small amount of mare basalts inside [11, 13], however, it is possible that more abundant mare basalt could be covered by ejecta from the surrounding crust.

Compensation Mechanism: The central gravity high of Type I basins in Bouguer anomalies suggests the existence of excess mass below the center. Because mare fill is absent from Type I basins, the central gravity high is most likely a manifestation of mantle uplift beneath the basin. The magnitude of the central high of Type I basins of 200 to 300 mGal corresponds to an undulation of the crust-mantle boundary of 10 to 15 km. Estimates of the depth after post-shock rebound of Type I basins from their diameters [14] are 3 to 4 km. This depth is too shallow for the central gravity high to be attributed to topographic relaxation of the basins. We therefore consider that the crust-mantle surface was overcompensated during shock event as proposed from a dynamic mantle rebound model [15].

The peak height of positive Bouguer anomalies of Type II ranges from 400 to 900 mGal in comparison to those in free-air anomalies from 250 to 500 mGal. This difference can be attributed to local compensation at the center of the Type II basins. As for the Type I basins, the concentric rings of positive and negative free-air anomalies suggests that rims and topographic depression of Type II basins is not compensated and is supported by a rigid lithosphere. Therefore neither the viscous relaxation nor the elastic compensation is plausible as mechanism of the central compensation of the Type II basins. We propose a brittle deformation resulting from a load of uplifted mantle. Mare volcanism is inferred as a result of fault system developed at the center of the Type II basins.

Little relation between the class and formation age is found. On the other hand, there are fewer large lunar basins on the far side. Type I and II basins tend to locate at the center of the far side and on the limb, respectively. It is unlikely that large impacts concentrated on one side of the Moon and smaller impacts on the other side, or that a thinner crust on the near side resulted in larger basins than on the far side, as crater diameter depends mostly on impacting energy and momentum, not the properties of the target [16]. A plausible hypothesis is that the primary mascon basins on the near side have deformed more after their initial formation. Tectonic ridges and troughs on the near side maria indicate that deformation continued after emplacement of mare basalt. The generally lower magnitude of the positive gravity plateau of primary mascon with respect to Type II basins further implies that not only the surface but also the crust-mantle boundary were relaxed.

References: [1] P. M. Muller and W. L. Sjogren, *Science*, **161**, 680 (1968). [2] F. G. Lemoine et al., *JGR*, **102**, 16,339, (1997). [3] A. S. Konopliv et al., *Icarus*, **150**, 1 (2001). [4] W. M. Kaula, *Theory of Satellite Geodesy* (1966). [5] B. G. Bills and A. J. Ferrari, *JGR*, **85**, 1013, (1980). [6] A. S. Konopliv et al., AIAA Astro. Spec. Conf., 93 (1993). [7] T. Iwata et al., *JGSJ*, **47**, 558 (2001). [8] N. Namiki et al., *LPSC XXXIX*, (2008). [9] N. Namiki et al., accepted by *Science* (2009). [10] H. Araki et al., submitted to *Science* (2009). [11] J. L. Whitford-Stark, *Moons Planets*, **26**, 323 (1982). [12] M. J. S. Belton et al., *Science*, **255**, 570 (1992). [13] D. E. Wilhelms et al., *The geologic history of the Moon* (1987). [14] R. J. Pike, *Proc. LPSC*, **8**, 3427 (1977). [15] G. A. Neumannet al., *JGR*, **101**, 16,841 (1996). [16] H. J. Melosh, *Impact Cratering: A Geologic Process* (1989).

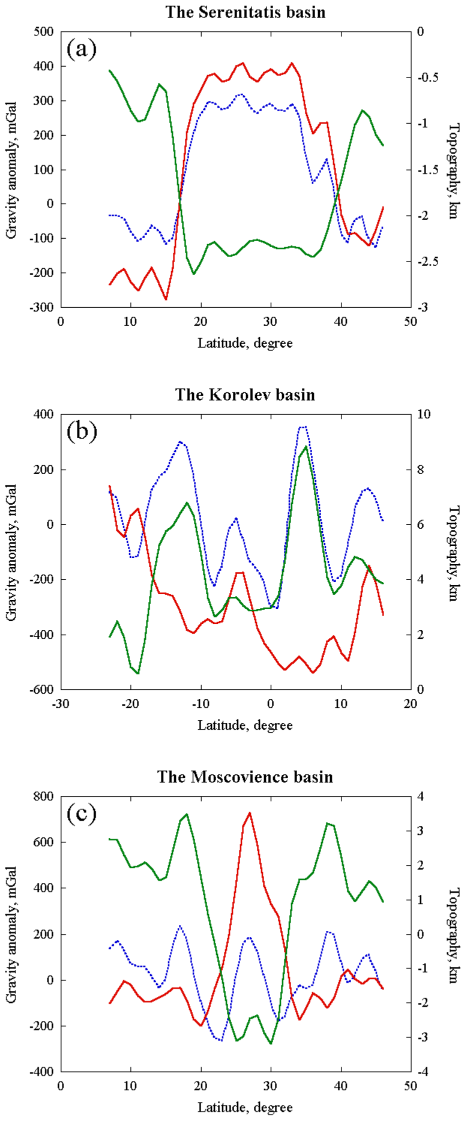

Fig. 1. Cross sections of gravity and topography of (a) the Serenitatis, (b) the Korolev, and (c) the Moscoviense basins. Free-air gravity anomalies, Bouguer gravity anomalies, and topography along longitudinal line are shown by blue, red, and green lines, respectively.